chloroform. Nevertheless, the T_1 value for the *tert*-butyl protons in this system is reduced from 3.2 to 0.8 s, suggesting that a complex is formed but that it is different in structure from the ones that exist in the more polar solvents.

Experimental Section

Determination of Dissociation Constants for Calixarene–Amine Complexes. In a typical determination a 0.0542 M solution of *p*-allylcalix-[4]arene in CD_3CN was used to prepare solutions containing measured excesses of *tert*-butylamine. The ^1H NMR spectra were measured on a JEOL FX-100 spectrometer, using 200 scans with a 90° pulse and a 14 s delay. The concentration of the amine in a given solution was determined by a comparison of the integrated intensity of its methyl resonance with that of the aryl resonance of the calixarene.

Determination of Relaxation Times (T_1). Solutions of *p*-allylcalix-[4]arene (0.005 M) in CD_3CN containing various concentrations of *tert*-butylamine were degassed at 0.1 mmHg pressure with six freeze–thaw cycles. The T_1 values of the proton resonances were obtained at 100 MHz and 25 °C by using the inversion recovery method.[41] To determine the T_1 of a given resonance a series of 11 spectra (each consisting of 25–100 scans) was obtained by using 180°–τ–90° pulse sequences with a delay of 5 times T_1 between pulse sequences. The time between pulses (τ) was varied between 0.5 and 1.5 times the T_1. The T_1 values were determined from semilogarithmic plots of the intensity of the resonance vs. τ. In all cases the deviation from linearity was less than 0.0005 s; the T_1 values are accurate to ±0.01 s.

(41) Vold, R. L.; Waugh, J. S.; Klein, M. P.; Phelps, D. E. *J. Chem. Phys.* **1968**, *48*, 3831.

Proposed Structure of Heme *d*, a Prosthetic Group of Bacterial Terminal Oxidases

Russell Timkovich,*† Margaret S. Cork,† Robert B. Gennis,‡ and Peter Y. Johnson†

Contribution from the Department of Chemistry, Illinois Institute of Technology, Chicago, Illinois 60616, and the Departments of Chemistry and Biochemistry, University of Illinois, Urbana, Illinois 61801. Received February 5, 1985

Abstract: Heme *d* has been isolated from the purified terminal oxidase complex of *Escherichia coli* strain MR43L/F152. After conversion to the metal-free methyl ester form, termed chlorin *d*, its structure was investigated. It was determined to be a chlorin, that is, a porphyrin with one pyrrole ring saturated so that the β carbons have sp^3 hybridization. Substituents were identified by means of visible, infrared, mass spectrometric, and ^1H NMR spectroscopy. The configuration of substituents was assigned by means of nuclear Overhauser enhancements between nearest neighbors and by the differential effects of a lanthanide shift reagent. The proposed structure of chlorin *d* contains the substituents 1-methyl, 2-vinyl, 3-methyl, 4-vinyl, 5-methyl, 5-hydroxyl, 6-(γ-lactone), 7-propionyl methyl ester, and 8-methyl. Ring C is the saturated pyrrole, and the 6-substitutent is an unusual spiro-γ-lactone.

In 1928 a pigment was observed in cells of *E. coli* and *Shigella dysenteriae* grown aerobically that appeared to be an unusual cytochrome with a pronounced red shift of the α band of the visible spectrum to the 630-nm region.[1] Further work on the respiratory electron transport chain of certain bacteria confirmed the existence of this cytochrome which came to be called cytochrome a_2. It has been detected in diverse bacteria including *Azotobacter*, *Proteus*, *Acetobacter*, *Salmonella*, *Bacillus*, *Pseudomonas*, and *Haemophilus*. By in vivo experiments as well as isolation and characterization of purified enzymes, the function of cytochrome a_2 was established. It functions in the aerobic respiratory metabolism of certain bacteria as a terminal oxidase reducing oxygen to water. Since about 1970, this cytochrome and its prosthetic group heme have been termed cytochrome *d* and heme *d* to avoid confusion with cytochrome aa_3 and the prosthetic group heme *a*, because it became clear that different chemical structures pertained.

In 1956 Barrett[2] proposed a structure for heme *d* as the Fe chelate of 7,8-dihydroprotoporphyrin IX, with some ambiguity as to whether the 2,4-vinyl groups were instead hydroxyethyl groups. This proposal was based upon derivatization chemistry as well as comparisons of chromatographic behavior and visible spectra with models. The main source of material was cells of *Aerobacter Aerogenes*, but chromatographic and visible spectral comparisons indicated that the pigment was identical with that found in *Azotobacter vinelandii*, *Escherichia coli*, *Proteus vulgaris*, *Bacillus subtilis*, and *Pseudomonas aeruginosa*.

Several considerations have prompted a fuller structural investigation on heme *d*. A deeper understanding of the terminal oxidase function of the host enzyme will require precise structural features for the prosthetic group active site. A recent structure determination on heme d_1 from bacterial dissimilatory nitrite reductases revealed that heme d_1 possesses a novel structure very

† Illinois Institute of Technology.
‡ University of Illinois.
* To whom correspondence should be addressed at the following present address: Department of Chemistry, University of Alabama, P.O. Box H. University, AL 35486.

(1) A review of the history of cytochromes *d* with references to the original literature may be found in the following: Lemberg, R.; Barrett, J. "Cytochromes"; Academic Press: New York, 1973; pp 8–14 and 233–240. In this paper the following terminology will be employed. "Heme" is a general term referring to the iron chelate form regardless of the oxidation state of either the central iron or the organic macrocycle. "Chlorin" refers to a porphyrin with one pyrrole that has been saturated so that the β carbons are now quaternary. "Protoheme" refers to Fe protoporphyrin IX without implying any information about the Fe oxidation state or the identity of axial ligands. "Heme *b*" is a general term for a noncovalently associated prosthetic group that characteristically gives an α band in the ferrous state near 560 nm. It is often taken as synonymous with protoheme, but in fact, this requires structural confirmation. "Cytochrome" refers to a heme associated with a polypeptide chain, whether the polypeptide is a stand alone protein or a subunit of a complex enzyme.

(2) Barrett, J. *Biochem. J.* **1956**, *64*, 626–639.

6070 *J. Am. Chem. Soc., Vol. 107, No. 21, 1985*

Timkovich et al.

Ia, R = CH₃
Ib, R = C²H₃
Ic, R = H

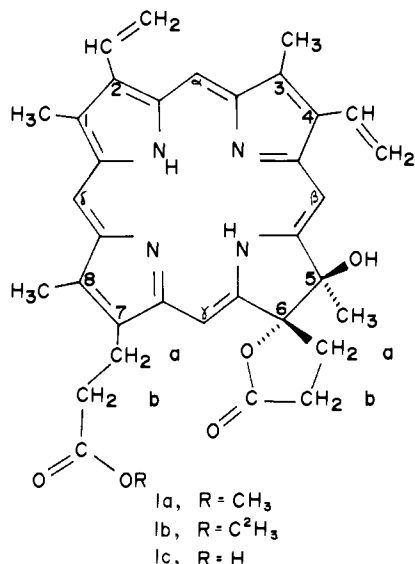**Figure 1.** Proposed structure for chlorin *d*, the organic macrocycle isolated from heme *d*, with a substituent labeling scheme.

Figure 2. (Left, A) visible absorption spectrum of *E. coli* heme *d* in chloroform, 25 °C, after chromatography on silica gel as described in the text. (Right, B) visible absorption spectrum of the metal-free, methyl ester derivative of heme *d* in chloroform, 25 °C. Band maxima are noted on the spectra.

distinct from other porphyrins.[3] At one time it had been thought that hemes *d* and d_1 were structural homologues based upon their visible spectra. The results for heme d_1 showed that unusual porphyrin substituents can appear in bacterial hemes and their existence is not always evident from the visible spectrum. Barrett's pioneering studies were limited by the techniques then available. The purpose of this report is to present evidence from spectroscopic studies that include visible, infrared, mass spectrometry, and high-field ¹H NMR that reveals a structure quite distinct from the previous proposal.

The heme *d* containing terminal oxidase complex from *E. coli* has recently been purified to homogeneity and characterized.[4,5] The membrane-solubilized oxidase complex is composed of two types of polypeptides with molecular weights of 57 000 and 43 000, with the best current data indicating a 1 to 2 stoichiometry of the two subunits in the native functional enzyme.[6] The complex does not contain significant amounts of acid-labile sulfur, non-heme iron, copper, or flavin. Three distinct heme prosthetic groups are evident in the visible spectrum of the enzyme: heme *b*-558, heme *d*, and an unusual heme a_1 that appears as a 595-nm band in the visible spectrum of dithionite-reduced enzyme. The heme content of *b*-558 and a_1 has been difficult to determine because of unusual extinction coefficients, and the current hypothesis is that heme a_1 is actually a high-spin heme *b* similar to that found in cytochrome *c* peroxidase.[6] There are two hemes *d* per complex, and they are identified as the oxygen-active sites by midpoint potential and ability to complex carbon monoxide. This terminal oxidase complex has been used as source material for the isolation of heme *d* and subsequent spectroscopy because of its relative ease of purification and very high yields of heme *d* and the fact that the host enzyme has been well defined.

Results

The proposed structure of the organic skeleton of heme *d* is shown in Figure 1 with a conventional labeling scheme to aid in the ensuing discussion. It must be stressed that with the exception of the visible spectrum of extracted heme *d*, the spectral analyses focused on the metal-free, esterified forms **1a,b** for reasons to be discussed. From the structures of **1a,b** one infers that the structure of heme *d* will correspond to the iron-chelated form of **1c**, the free carboxylic acid form. The relation between the structures of **1a,b**
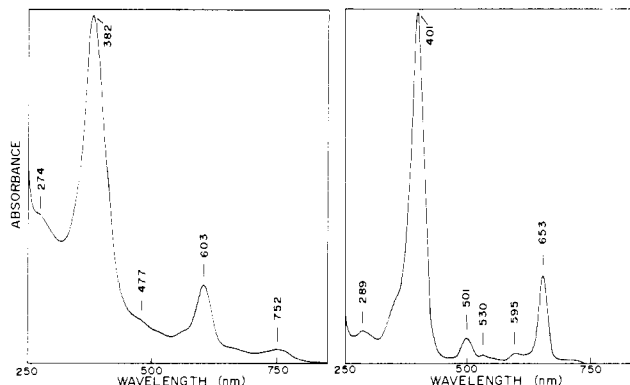
and the true enzyme bound form of heme *d* will be treated at length in the Discussion.

Extraction of heme *d* and Conversion to the Metal-Free Porphyrin. The success of this project ultimately relied upon the high levels of the terminal oxidase in the *E. coli* strain MR43L/F152, which contains the F152 episome.[7] Whole cells contained on the order of 10 μmol of heme *d* per 100 g of wet weight, and at this level the cells are a dark green in appearance. Attempts to isolate and purify the heme from whole cells or membrane fragments were never fully successful because of a pronounced tendency of the heme to aggregate with other hydrophobic constituents and a marked lability of the heme in crude extracts. The former had been previously noted by Barrett[2] and may account for some of the chromatographic behavior observed in his preparations. Isolation of heme *d* required purified oxidase. The heme extract prepared from the oxidase complex was still insufficiently pure for detailed spectroscopic analysis. This type of difficulty has been noted in other heme structural studies.[3,8] Furthermore, in the initial extract the heme is exceedingly labile, even under darkened, anaerobic conditions. The lability presumably accounts for an earlier report on an inability to detect heme *d* in extracts from the purified oxidase.[4] In principle, one could obtain meaningful structural results by studying low-spin ferric or diamagnetic ferrous complexes of purified heme with strong field ligands, such as the bis-cyano complex. However, there are unique features to the coordination chemistry of heme *d* that would complicate a structural analysis,[9] and the complexes are still quite labile. Therefore, definitive structural results were sought on a stabilized form of the macrocycle, **1a,b**. This required removal of the central iron, esterification of any carboxylic acid groups, and subsequent purifications. Although the overall yield of these steps was poor, the final product was homogeneous, stable, and amendable to unambiguous spectroscopic analysis.

The visible spectrum of ferric heme *d* in chloroform after silica gel chromatography is shown in Figure 2A. Barrett used the ratio of absorption at 603 nm (due to heme *d*) to absorption at 635 nm (due to protoheme and other contaminants) as an indication of purity. His best preparations had a ratio of 2.86, while ours consistently showed ratios in excess of 3.9 with a high of 4.37. Band maxima were in agreement for heme *d*, its complexes as reported by Barrett[2] and the iron-free form. The spectrum of the iron-free methyl ester derivative **1a** is shown in Figure 2B. The pronounced bands at 603 nm for the heme and 649 nm for **1a** are characteristic of porphyrins reduced to the level of chlorins by saturation of one β-pyrrolic double bond. The spectra bear

(3) Timkovich, R.; Cork, M. S.; Taylor, P. V. *J. Biol. Chem.* **1984**, *259*, 1577–1585.
(4) Miller, M. J.; Gennis, R. B. *J. Biol. Chem.* **1983**, *258*, 9159–9165.
(5) Koland, J. G.; Miller, M. J.; Gennis, R. B. *Biochemistry* **1984**, *23*, 1051–1056.
(6) The stoichiometry of the subunits, the spectral analysis of the unusual heme a_1, and the heme *d* content will be the subject of a future manuscript. Lorence and Gennis, in preparation.

(7) Shipp, W. S.; Piotrowski, M.; Friedman, A. E. *Arch. Biochem. Biophys.* **1972**, *150*, 473–481.
(8) Murphy, M. J.; Siegel, L. M.; Kamin, H.; Rosenthal, D. *J. Biol. Chem.* **1973**, *248*, 2801–2814.
(9) A study of the coordination chemistry of heme *d* with exogenous ligands is in progress and will be the subject of a future report.
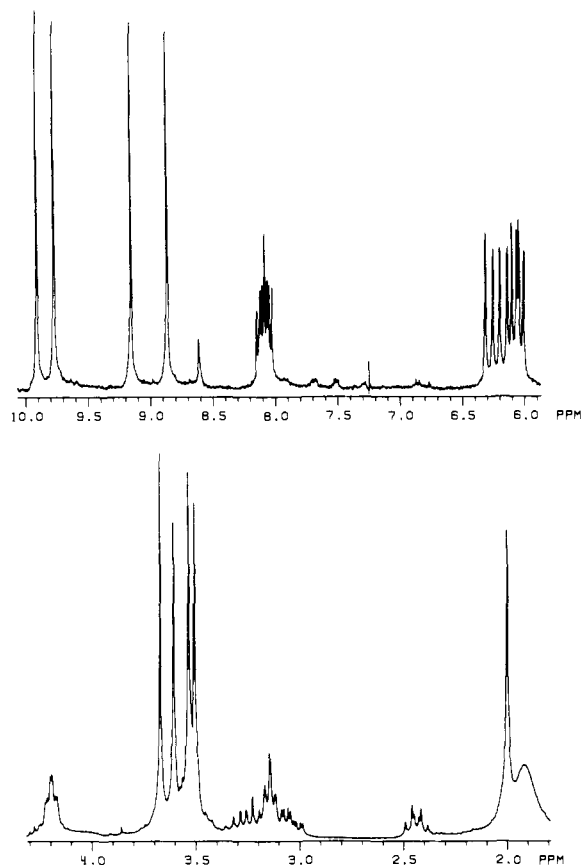
Figure 3. ^{1}H NMR spectrum of the metal-free, methyl ester derivative **1a** of *E. coli* heme *d* at 25 °C, in C^{2}HCl$_3$ at 300 MHz. The spectrum is presented in parts so that the effects of spin coupling, which were critical for the structural analysis, may be more readily discerned. The vertical scales of the two regions shown are not the same, but they have been adjusted for a convenient display. The broad peak at circa 1.9 ppm is believed to be residual water and ranged from 1.5 to 1.9 ppm depending upon the moisture content of the sample and NMR solvent. Additional features not shown are the pyrrolic NH resonance at –2.251 ppm and solvent impurities at 1.2 and 0.8 ppm.

similarities to hydroxyl-containing porphyrins and chlorins previously synthesized,[10–12] but in the absence of systematic and extensive model studies of the interplay of other substituents with the visible spectra, the importance of the similarity is difficult to judge.

Identification of Substituents. The metal-free chlorin contained one free carboxylic acid. Comparison of the ^{1}H NMR in the methyl ester region for the methyl ester derivative **1a** prepared with protic reagent vs. the ester derivative **1b** prepared with deuterated diazomethane showed that the spectra differed only in the disappearance of one methyl singlet at 3.663 ppm. This also served to assign the methyl ester resonance. In confirmation of this assignment, this ester resonance experienced one of the largest landthanide-induced chemical shifts, consistent with its proximity to the carbonyl lanthanide binding site that will be discussed later. Low-resolution mass spectral comparison of **1a** and **1b** indicated that the molecular ion of the deuterated compound was three mass units higher than that of the protic, confirming one free carboxylate and indicating that the diazomethane treatment did not lead to any other addition products.

The 300-MHz ^{1}H NMR spectrum of **1a** is shown in Figure 3. Spectral parameters and assignments are given in Table I. Most of the spin systems are readily recognizable as substituents on unsaturated pyrrole rings by their characteristic chemical shifts,
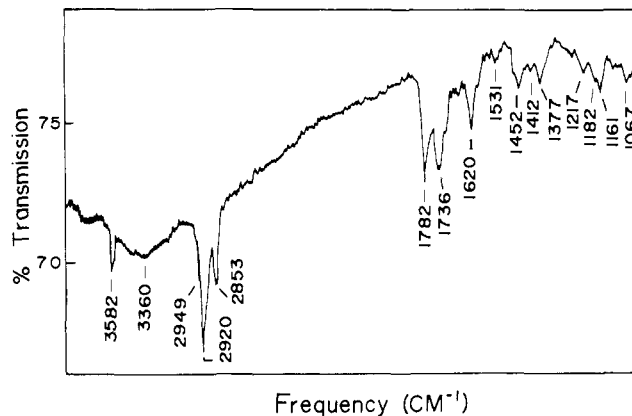

Figure 4. Fourier transform IR spectrum of the chlorin methyl ester **1a**. The sample was a dried film between NaCl disks. Peak maxima are indicated. Critical features pertinent to the structural investigation are the hydroxyl modes at 3582 and 3360 cm^{-1} and the lactone carbonyl mode at 1782 cm^{-1}.
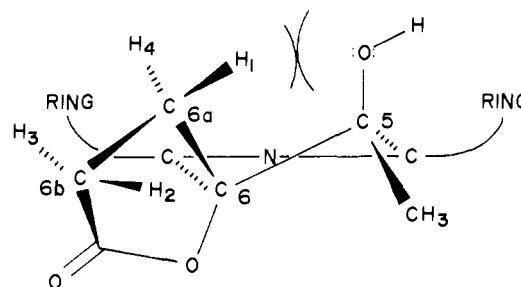

Figure 5. Proposed substructure of the saturated pyrrole in heme *d*. A front view showing H, OH van der Waals steric compression resulting from the pyrrole half-chair conformation.

intensities, and coupling constants.[13] The observation of four meso proton singlets confirms that the meso positions are unsubstituted, and their relatively upfield chemical shifts and pronounced grouping into two pairs is characteristic of chlorins and confirms the conclucions reached from the visible spectra.

Assignment of the remaining substituents, which must be on the saturated pyrrole because all other positions have now been assigned, is not straightforward and requires consideration of other spectroscopic data. Remaining ^{1}H NMR features are the three proton singlet at 1.995 ppm, the one proton multiplet at 2.431 ppm, and the complex multiplet representing three protons spanning the 3.00–3.25 ppm region. The chemical shift of the 1.995-ppm resonance is characteristic of a methyl group on a saturated pyrrole. Its appearance as a singlet means there is no strong ^3J coupling to the other substituent at the quaternary pyrrolic carbon. There is no known precedent in porphyrin NMR for the remaining multiplets.

High-resolution mass spectrometry established the empirical formula of **1b** (obsd 595.2858 and calcd 595.2876 for C$_{35}$N$_4$O$_5$H$_{33}$D$_3$). Considering the assigned structural fragments, the remaining substituents on the saturated pyrrole must account for C$_3$H$_5$O$_3$. The infrared spectrum (Figure 4) gave expected chlorin modes, but it also afforded evidence for the saturated pyrrolic substituents. The broad mode at 3360 cm^{-1} with a sharp spike at 3582 cm^{-1} is characteristic of hydroxyl groups. The carbonyl region showed a typical propionyl ester at 1736 cm^{-1} and a second mode at 1782 cm^{-1}. This latter mode is characteristic of γ-lactone carbonyls or strained cycloalkanones.

The observed multiplets at 2.431 and 3.00–3.25 ppm were successfully simulated as an ABCM subspectrum with the shifts
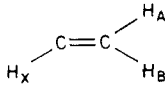
(10) Inhoffen, H. H.; Nolte, W. *Liebigs Ann. Chem.* **1969**, *725*, 167–176.
(11) Inhoffen, H. H.; Schwarz, N.; Heise, K. P. *Liebigs Ann. Chem.* **1973**, 146–160.
(12) Bonnett, R.; Dimsdale, M. J.; Stephenson, G. F. *J. Chem. Soc. C* **1969**, 564–570.

(13) A bibliography of porphyrin NMR literature has been cited in ref 3. Most of the spectrum of Figure 3 is assignable by comparison to protoporphyrin IX dimethyl ester with the understanding that resonances in the chlorin are upfield from analogous spin systems in an unsaturated porphyrin because of a decrease in the effective ring current of the chlorin.

6072 *J. Am. Chem. Soc., Vol. 107, No. 21, 1985*

Timkovich et al.

Table I. ^{1}H NMR Assignments for Chlorin d

assignment[a]	chemical shift[b]	protons[c]	coupling[d]
meso α	9.902	1	s
meso β	9.145	1	s
meso γ	8.856	1	s
meso δ	9.764	1	s

2, 4 - vinyls[e]

X_i	8.091	2	$J(X_i,A_i) = 17.8$
X_j	8.091		$J(X_j,A_j) = 17.8$
A_i	6.104		$J(X_i,B_i) = 12.2$
B_i	6.297	4	$J(X_j,B_j) = 11.7$
A_j	6.164		$J(A_i,B_i) = 0.9$
B_j	6.023		$J(A_j,B_j) = 1.0$
propionate			
$-CH_2CH_2COOMe$ (**7a**)	4.188	2	$J(7a,7b) = 7.6$
$-CH_2CH_2COOMe$ (**7b**)	3.137	2	
$-CH_2CH_2COOMe$	3.663	3	
ring methyls			
1	3.499	3	s
3	3.599	3	s
5a	1.995	3	s
8	3.528	3	s
lactone[f]			
$6b_3$	3.231 (3.7)		$J(6a_1,6b_2) = 3.8$ (4.5)
$6b_2$	3.032 (3.4)	3	$J(6a_1,6b_3) < 2$ (0.5)
$6a_1$	3.169 (3.2)		$J(6a_1,6a_4) = -13.0$ (-12.4)
$6a_4$	2.431 (2.4)	1	$J(6b_2,6b_3) = -16.9$ (-15)
			$J(6b_2,6a_4) = 9.6$ (9.5)
			$J(6b_3,6a_4) = 9.6$ (8.0)
pyrrole NH	-2.251	2	s, br

[a] Resonances have been labeled according to the scheme shown in Figure 1. [b] Chemical shifts are in ppm for 25 °C in C^{2}HCl$_3$. [c] Average areas rounded to the nearest integer assuming that the meso resonances represent one proton each per molecule. For overlapping multiplets, the total area of the pattern is given. [d] Singlets are designated as s. Other values are in Hz obtained from direct observation (J(7a,7b)) or as the result of computer simulation. [e] Vinylic resonances appear as two intermixed ABX type of subspectra that were analyzed by simulation with the shifts and coupling constants as reported and have been labeled $A_iB_iX_i$ and $A_jB_jX_j$. These would correspond to the vinyls at substituent positions 2 and 4, but it has not been possible to assign which is which. [f] The assignment of the methylene protons of the lactone has been discussed in the text. The labeling scheme is as follows. The protons $6a_1$ and $6a_4$ are the geminal protons on the first carbon bonded to the pyrrole and $6b_2$ and $6b_3$ are the geminal protons on the next carbon out. Protons $6a_1$ and $6b_2$ point toward the 5-OH and $6b_3$ and $6a_4$ point away. The values given in parentheses are the predicted chemical shifts and coupling constants based upon the model described in detail in the text. The chemical shift predictions for protons $6b_2$ and $6b_3$ are high because a fully unsaturated porphyrin ring current was employed to calculate deshielding contributions. In a chlorin, the ring current is diminished for the macrocycle as a whole, but especially in the immediate vicinity of the saturated pyrrole, leading to decreased deshielding contributions. To our knowledge, a quantitative ring current calculation for a chlorin with significant out of plane substituents has not been made.

and coupling constants reported in Table I.

Numerous substructures were considered to account for the $C_3H_5O_3$ fragments. The preferred substructures, a spiro-γ-lactone and a hydroxyl, were found to be in accord with the observed data, including the unusual 1782-cm^{-1} mode and the hydroxyl modes at 3582 and 3360 cm^{-1} in the IR spectrum. The NMR assignments of the four protons on the C_3 fragment were based on

analysis of their predicted chemical shifts and coupling constants as outlined below. First, inspection of models indicated that the most stable conformation for the proposed trans spirolactone would have the bulkier 5-methyl group and methylene carbon 6a of the spirolactone group in a pseudoequitorial arrangment (Figure 5) and that the macrocyclic ring would be nearly planar. Second, it was assumed that two major factors would have an effect on the chemical shift of the C_3 fragment's protons. These are (1) the anisotropic shielding effects due to the ring current associated with the macrocyclic ring and (2) the van der Waals steric compression effects due to the close proximity of H1 on carbon 6a of the spirolactone to the cis hydroxyl group on the carbon 5 of the pyrrole ring (Figure 5). The magnitude of the chlorin ring current was approximated by assuming the isoshielding lines of chlorins are similar, though slightly diminished, to those published for fully unsaturated porphyrins.[14] This assumption was tested with good success against published chlorin NMR spectra. By measuring the distance on models of the spirolactone protons from the center of the ring (out) and their height above the plane of the ring (up), it was estimated that protons H2 (ca. 7.3 Å out, 0.5 A up) and H3 (ca. 6.5 Å out, 0.7 Å up) next to the lactone carbonyl would be deshielded by 1.0 and 1.3 ppm, respectively. Assuming a base of 2.4 ppm for methylene protons next to a carbonyl, one predicts chemical shifts for H2 and H3 of 3.4 and 3.7 ppm, respectively. Applying the same treatment to protons H1 (ca. 6.0 Å out, 1.4 Å up) and H4 (ca. 5.1 Å out, 1.2 Å up) leads to deshielding of 1.3 and 1.4 ppm, respectively. Assuming a base of 1.2 ppm for normal methylene protons, chemical shifts of 2.5 and 2.6 ppm would be predicted for H1 and H4 on carbon 6a. These two protons are also expected to have their respective chemical shifts affected by the close proximity of the neighboring hydroxyl group on carbon 5 (see Figure 5).[15,16] Models of the spirolactone containing chlorin indicate that H1 and the oxygen of the adjacent hydroxyl group are approximately 2.6 Å apart. Calculation of the van der Waals contribution to the chemical shift of H1 and H4 (see eq 3.1),[17] which results from electron reorganization about H1 and H4 due to the hydroxyl oxygen's electron density, indicates that H1 will be deshielded by 0.7 ppm while H4 will actually be shielded by 0.2 ppm. These added corrections suggest final chemical shifts in the range of 3.2 ppm for H1 and 2.4 ppm for H4. The coupling constants expected for this spirolactone system are similar to those determined by spectrum simulation. Puckering the five-membered-ring lactone (half-chair) so as to leave the carbonyl pointed away from the cis methyl on the saturated chlorin ring and viewing the lactone down the CH_2-CH_2 bond shows that the methylene protons are nearly eclipsed. Using Karplus relationships[18] for predicting geminal and vicinal coupling constants results in the following conclusions. First, the geminal coupling between H2 and H3 is expected, because of π-electron withdrawal due to the carbonyl, to be more negative than the standard value of -12.4 Hz found for typical methylene groups. For example, J is -15 Hz for acetone and becomes even more negative in some rigid systems.[17] Simulation required $J_{2,3}$ to have a value of -16.9 Hz. Geminal coupling between H1 and H4 is expected to be typical (simulation required $J = -13$ Hz). The dihedral angles between the protons on the adjacent methylene carbons are expected to be skewed because of the steric compression between H1 and the nearby hydroxyl group. Given this interaction, the following dihedral coupling constants are predicted. For H1,H2 (ca. 40°), $J = 4.5$ Hz. For H1,H3 (ca. 100°), $J = 0.5$ Hz. For H4,H2 (ca. 160°), $J = 9.5$ Hz. For H4,H3 (ca. 20°), $J = 8$ Hz. These values are in good qualitative agreement with the simulated dihedral coupling constants. Table I summarizes the simulated and predicted data. We

(14) Scheer, H.; Katz, J. J. In Porphyrins and Metalloporphyrins"; Smith, K. M., Ed.; Elsevier: Amsterdam, 1975; pp 402.

(15) Yonemoto, T. *Can. J. Chem.* **1966**, *44*, 223–227.

(16) Fukunaga, T.; Clement, R. A. *J. Org. Chem.* **1977**, *42*, 270–275.

(17) Lambert, J. B.; Shurvell, H. F.; Verbit, L.; Cooks, R. G.; Stout, G. H. "Organic Structural Analysis"; Macmillan: New York, 1976; p 5098.

(18) Silverstein, R. M.; Bassler, G. C.; Morril, T. "Spectroscopic Identification of Organic Compounds", 3rd. ed.; Wiley: New York, 1974; p 91.
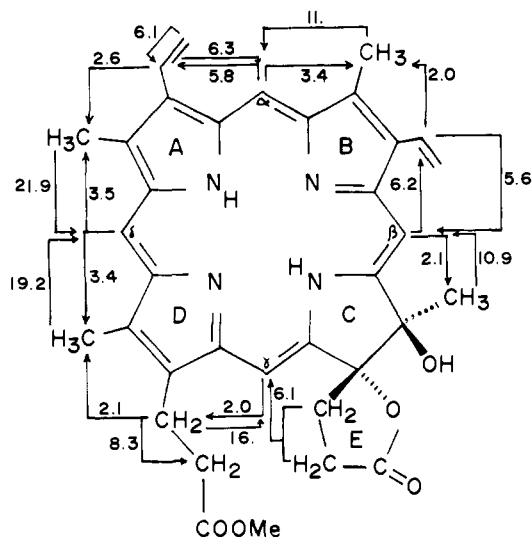
Figure 6. Observed nuclear Overhauser enhancements between the resonances of the chlorin methyl ester **1a**. The dotted arrows indicate that a positive enhancement was observed. The base of the arrow indicates which resonance was irradiated, and the head of the arrow indicates which resonance was observed. The value given along the arrow is the percent enhancement. Resonances for the two vinyl substituents overlap, and it was not possible to assign which one, or whether both, gave the observed enhancement of 6.1% across the double bond illustrated for display purposes at position 2. Also because of overlap it was not possible to assign which proton was responsible for the enhancement of 6.1% from the lactone ring methylene protons to the γ-meso proton.

were unable to find another three-carbon substructure which fit these data.

Configuration of Substituents. The relative placement of substituents about the macrocycle was determined by observation of nearest neighbor nuclear Overhauser enhancements (NOE's) and differential lanthanide induced chemical shifts (LIS's).[19] Observed NOE's are reported schematically in Figure 6. For a relatively rigid macrocycle like **1a** NOE's are expected only between nearest neighbor protons. By investigating NOE's for all resolved spin systems, one builds up a pattern of neighbors that is consistent with only one configuration of substituents. For example, irradiation of the meso proton at 9.764 ppm gave NOE's to only two methyl resonances at 3.499 and 3.528 ppm, establishing these as adjacent to the meso proton. Irradiation of the vinylic protons at 8.1 ppm gave NOE's to the 3.499 ppm methyl and the 9.902 ppm meso resonances, establishing them as adjacent and building up the configuration of substituents as shown in Figure 6. Unfortunately, not all possible NOE's have been observed, because some enhancements may be below the current observation limit of 2%. Because of the spread of the multiplets arising from the lactone ring, it was not possible to ascribe an NOE to the adjacent meso proton at 8.856 ppm as originating from a specific methylene proton(s). However, sufficient NOE's and confirming reciprocal NOE's have been observed so that the total pattern is only consistent with the configuration assigned.

Lack of an NOE between the methyl at 1.995 ppm and any lactone ring protons is weak but confirming evidence for the trans configuration previously assigned on the basis of chemical shift considerations. If the methyl and methylene groups were cis, the close proximity (circa 2 Å) should have allowed an observable NOE, while in the trans configuration the average distance is >4 Å and an only a weak enhancement would have been possible at best.

Figure 7 schematically presents the effects of lanthanide-induced shifts reported as the equilibrium binding constant times the bound state chemical shift, $K\omega$. Justification for this method has been given previously.[19] Larger values indicate closer proximity to the
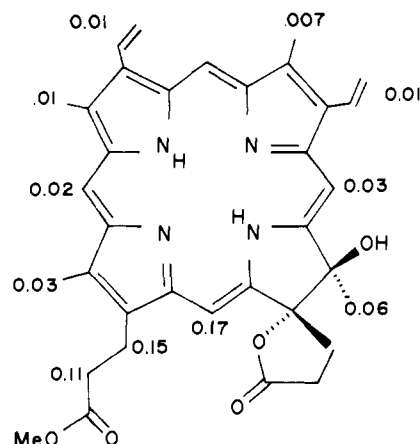

Figure 7. Observed values for the equilibrium binding constant times the bound state chemical shift ($K\omega$) for the resonances of the chlorin methyl ester **1a** in the presence of a lanthanide shift reagent. Values are given next to the corresponding proton spin system on the structural diagram. The resonances of the lactone could not be followed because of overlap with the shifting ring methyls and propionate methylenes and because the small but significant line broadening introduced by the shift reagent made the weak multiplets unobservable. Similar line-broadening problems only allowed an upper estimate to be made for the vinyl resonances.

Scheme I
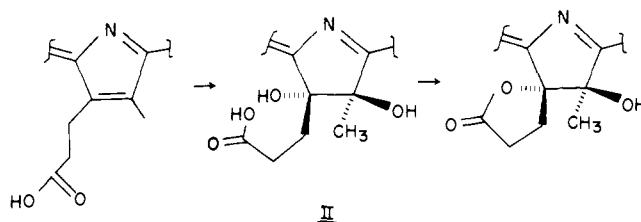
lanthanide-binding site. The total pattern is consistent with the lanthanide reagent binding in the vicinity of the carbonyls, as has been found for other porphyrins.[19] Since the substituents are largely constrained to the plane of the macrocycle, the distances reflected in values of $K\omega$ are evidence for the assigned configurations.

Discussion

Two enzyme prosthetic groups have now been characterized that contain two sp³ β-pyrrolic carbons, and it is unfortunate that in the biochemical literature they have been termed heme *d* and heme d_1. They have very different substituents and the location of the saturated pyrrole is different. In heme d_1, it is a non-propionate-containing pyrrole ring that is saturated, while in heme *d* it is ring C with a substructure that may well be derived from a propionate substituent.

The deduced structure leaves unanswered the question of the absolute configuration (*R* or *S*) about the quaternary carbons of the saturated pyrrole. But the present interpretation of the data makes a firm prediction that the carbon–oxygen bonds are in the trans configuration. The key is that of the four methylene protons associated with the saturated pyrrole, three are downfield of 3 ppm and only one is circa 2.4 ppm, leading to the ABCM subspectrum. This has been interpreted as arising from the electron reorganization about H1 and H4 due to the proximity of the hydroxyl oxygen. This is only possible in the trans configuration. Any alternative configuration would lead to an ABMN type of subspectrum. Although by itself the absence of an NOE between the adjacent methyl and these same methylene protons would not be compelling evidence, it does provide some confirmation that the assigned configuration is correct.

Spirolactone moieties have been previously encountered as microbial natural products, but this is the first instance of such a moiety in a porphyrin, natural or synthetic. Since lactones can form spontaneously under appropriate conditions, there is the possibility that the γ-lactone of chlorin *d* formed during workup

(19) Timkovich, R.; Cork, M. S.; Taylor, P. V. *J. Biol. Chem.* **1984**, *259*, 15089–15093.

from the crude heme extract from a diol precursor such as II in Scheme I. Attempts are in progress to investigate this possibility by direct spectroscopic analysis on heme *d*. However, the structural analysis of chlorin *d* still serves to establish the basic skeleton of heme *d*.

The structure of chlorin *d* strongly suggests that heme *d* is biosynthesized by a late modification of the general metabolic pathway for protoporphyrin IX. Indeed, this strain of *E. coli* is fully capable of the biosynthesis of protoporphyrin IX. Protoheme from the heme *b* prosthetic group of the terminal oxidase was isolated during the purification of heme *d* and converted into protoporphyrin IX dimethyl ester by standard methods.[20] It was identified as authentic on the basis of its characteristic visible and NMR spectra.[13] Chlorin *d* could arise from protoporphyrin IX by the hypothetical Scheme I, that proposes enzymatic hydroxylation of the pyrrole to form a diol, followed by enzymatic or non-enzymatic cyclization to form the spirolactone.

Although the visible and infrared spectra of heme *d* are not suitable by themselves for a de novo proof of structure, they are appropriate for comparisons. There is rich detail in the visible spectra of hemes in terms of precise band maxima, shapes, and relative intensities, and, if hemes from different sources match, then this is good evidence for structural homology. Thus it is likely that the *E. coli* heme *d* discussed here is identical with the pigments called heme *d* or heme a_2 found widely distributed in other bacterial systems.

Experimental Section

Spectroscopic Methods. Optical spectra were obtained on a Perkin-Elmer Lamda 5 spectrophotometer operating with 2-nm slits. Infrared spectra were obtained with a Nicolet FT-IR 5MX spectrometer with 4-cm^{-1} resolution. Solid thin-film samples for FT–IR were prepared by evaporating a dried chloroform solution of the chlorin onto NaCl disks which were further dried in a vacuum desiccator over KOH. One interferrogram was accumulated per second, and signal to noise was not improved beyond 6 h of averaging. ^{1}H NMR spectra were obtained on a Nicolet spectrometer operating at 300 MHz for protons in the Fourier transform mode. Routine spectra at 25 °C in a temperature-controlled probe for 5-mm tubes were obtained in 16 000 data point blocks by using quadrature detection with phase cycling and a 90 degree observation pulse. One transient was collected every 3.5 s, and preliminary spin lattice time measurements indicated this was greater than $5T_1$ for the slowest relaxing protons. Chemical shifts are reported in parts per million, nominally vs. tetramethylsilane. Residual C[1]HCl$_3$ in the deuterated chloroform solvent was used as the actual internal standard and assigned a chemical shift of 7.240 ppm. All NMR solvents were Gold label grade obtained from Aldrich. Peak areas were quantitated by standard Nicolet integration routines. Values reported represent averages over many spectra rounded to the nearest integer. Typical actual results were usually within 10% on the reported integer. The well-resolved meso protons, whose areas were 1:1:1:1, were taken as internal standards whose measured areas corresponded to one proton per molecule. Multiplet spectra were simulated by trial and error with use of the Nicolet software routine NICSIM. Measurements of nuclear Overhauser enhancements and lanthanide-induced shifts by tris(1,1,1,2,2,3,3-heptafluoro-7,7-dimethyloctane-4,6-dionato)europium(III) (commonly known as Eu(fod)$_3$) have been described.[19] All NOE's were positive and are expressed as the area of the enhanced resonance in difference spectra (with NOE minus a control) divided by the area in the control spectrum and converted to percent. The threshold for observation of an NOE was 2%. Lanthanide-induced shifts were measured in titration experiments where the range of added lanthanide was 0.5 to 50 mM. Slopes of these titration curves were converted into values of $K\omega$ were K represents the binding constant for the shift reagent to the chlorin and ω represents the shift in the bound state as previously described.[19] Mass spectra were obtained by using the fast atom bombardment technique at the Midwest Center for Mass Spectrometry, Department of Chemistry, University of Nebraska—Lincoln, with the assistance of Dr. K. B. Tomer. Samples handled by the Center were returned and re-examined by NMR to confirm the integrity of the samples during shipment and storage.

Isolation and Derivatization of Heme *d*. Culture conditions for *E. coli* strain MR43L/F152 and purification of the terminal oxidase have been described.[4] Typically cell paste in lots of 70–100 g wet weight was employed as starting material. All operations through the final HPLC

purification of the chlorin methyl ester were performed as rapidly as possible to minimize degradation. Several batches of the final methyl ester product, usually at least four, had to be pooled to obtain sufficient material for ^{1}H NMR spectroscopy, but independent batches over many preparations yielded indistinguishable spectra. The terminal oxidase after the chromatography step on DEAE-Sepharose CL-6b was suitable material for heme extraction. Attempts to extract the heme from material at an earlier state of purity or from whole cells were unsatisfactory. Yields were poor, the visible spectra had a high general background under the main heme chromophoric bands, and the heme aggregated with unidentified impurities that made further purification steps unfeasible.

Terminal oxidase (about 3 μmol) in buffer (200 mM KCl, 75 mM potassium phosphate, 5 mM EDTA, 6 mM Calbiochem Zwittergent 3–12, pH 6.3) was concentrated at 4 °C to 10 mL in an Amicon ultrafiltration cell with a PM-30 membrane under nitrogen. The following steps through the esterification were performed in a darkened room with solutions prechilled on ice-water baths. The concentrated protein solution was added dropwise to chilled acidic acetone (freshly made 2.1% (v/v) concentrated aqueous HCl in acetone, 2.4 mL per mL of protein solution) purged and agitated by a vigorous stream of nitrogen. The suspension was sealed under nitrogen in capped centrifuge bottles and centrigued to remove the precipitated apoprotein. The clear supernatant was extracted with cold ether that had previously been washed with aqueous ferrous sulfate to remove trace peroxides. The ether layer was dried with anhydrous magnesium sulfate under nitrogen, filtered, and dried in vacuo. The residue was extracted with small portions of ether, which preferentially solubiized heme *d* over heme *b* and other impurities, concentrated under a stream of nitrogen, and applied to a silica gel column (2.5 × 30 cm) equilibrated with dichloromethane. The column was eluted with the same until all the yellow lipid had come off, then with dichloromethane, methanol, and acetic acid (95:5:0.15). The emerald green heme *d* separated from protoheme which remained bound to the column. The green solution was dried under vacuum. Protoheme may be recovered from the column by increasing the eluent to 10% (v/v) or greater methanol. The extract before and after the preparative silica column was screened by thin-layer chromatography on silica plates developed with dichloromethane:methanol:acetic acid (3:1:0.05) (R_f 0.32 for heme *d* and 0.12 for protoheme). An important observation was that in no case was a third heme band, potentially the heme a_1 of the purified terminal oxidase, ever observed. This is additional evidence that the spectroscopically detected pigment a_1 in the native complex is either a heme *b* or a heme *d* with unusual optical bands, perhaps because of unusual axial ligand(s).

The crude dried heme *d* was redissolved in 5 mL of cold glacial acetic acid under nitrogen. With vigorous agitation, 0.1 mL of ferrous sulfate (10% w/v in concentrated HCl) was added. There was an immediate color change to a more bluish shade of green and spot tests showed the appearance of strong red fluorescence indicating iron removal. Within 1 min, the solution was poured into chilled ether, extracted with aqueous sodium acetate (20% w/v), and then washed with multiple portions of water. The ether solution was chilled on an ice-water bath, and a cold solution of diazomethane[21] was added dropwise with stirring. In preparations of the methyl-d_3 ester, deuterated diazomethane[22] in 1,2-dimethoxyethane–[2]H$_2$O was substituted. The reaction was monitored by spotting aliquots onto silica TLC plates and developing in 9:1 chloroform:ethyl acetate. The methyl ester (R_f 0.39) appeared as a strong orange-red fluorescent spot under ultraviolet light. The initial additions of diazomethane did not yield any product, due to consumption of diazomethane by residual acetate. Additions continued only until the yield of product was maximized, as judged by the fluorescence on the silica plates. Acetic acid (0.1 mL) was added to the crude ester solution to quench excess diazomethane and the solution concentrated in vacuo. It was applied to a short silica gel column (1 × 10 cm) and eluted with 9:1 chloroform:ethyl acetate. The ester was separated from non-mobile material that is believed to be degraded material produced during the demetallization. The ester solution was concentrated in vacuo, redissolved in a minimal volume of chloroform, and further purified by HPLC (conditions: Alltech column, 4.6 × 250 mm, 10 μm silica, room temperature, eluted with neat chloroform at 1 mL/min, detected optically at 400 nm). The major ester peak eluted with a capacity factor $k' = 3.75$ and was resolved from accumulated solvent impurities and minor porphyrin peaks that are believed to be products where the original vinylic side chains have been converted to hydroxyethyl substituents by the formal addition of H$_2$O across the double bond. Control experiments with iron protoporphyrin IX indicated that this side reaction occurs during the demetallization procedure. Ester fractions from several

(20) Fuhrhop, J. H.; Smith, K. M. In "Porphyrins and Metalloporphyrins"; Smith, K. M., ed.; Elsevier: Amsterdam, 1975; pp 757–869.

(21) Fieser, L. F.; Fieser, M. "Reagents for Organic Synthesis"; Wiley: New York, 1967; Vol. I, pp 191–193.
(22) Hecht, S. M.; Kozarich, J. W. *Tetrahedron Lett.* **1972**, *15*, 1501–1502.

batches were pooled, dried in vacuo, and stored in the dark at 4 °C. Optical and NMR spectra and rechromatography by HPLC indicated that the final product was stable when so stored. At the present time, accurate extinction coefficients for the metal-free methyl ester have not been obtained and the quantity of the ester can be estimated only from the intensity of NMR spectra. On the basis of this, the overall yield from the heme content of the terminal oxidase was estimated to be on the order of 10–20%. Major losses occurred in the initial acid–acetone extract and during the demetallization procedure.

Two-Step Covalent Modification of Proteins. Selective Labeling of Schiff Base-Forming Sites and Selective Blockade of the Sense of Smell in Vivo[1]

J. Russell Mason,[†] **Fah Che Leong,**[‡] **Kevin W. Plaxco,**[‡] **and Thomas Hellman Morton***[‡]

Contribution from the Monell Chemical Senses Center, Philadelphia, Pennsylvania 19104, and the Department of Chemistry, University of California, Riverside, California 92521. Received February 12, 1985

Abstract: Covalent modification by two-step labeling is illustrated by a blocker–fixer sequence, in which a protein forms a reversible complex with a blocker, which is then converted to an irreversible adduct by the fixer. When the Schiff base-forming enzyme, acetoacetate, decarboxylase (AAD), is used as an in vitro model, the blocker–fixer sequence is exemplified by ethyl acetoacetate (EAA) as the blocker and borohydride as the fixer. When reaction or removal of unbound blocker competes with protein labeling (e.g., with NaBH$_4$ as fixer), the quantitative expression for the extent of labeling is $\phi = 1 - (1 + \beta)^m$, where β is the ratio of the initial blocker concentration, S$_0$, to the dissociation constant for the reversible protein-blocker complex. This relationship is tested and demonstrated both for removal of the blocker by chemical reaction and for removal by dialysis. The value of the exponent m is a function of the reaction rate constants. The blocker–fixer sequence EAA–NaBH$_3$CN is shown to be specific for Schiff base-forming sites. Application of this blocker–fixer sequence to the olfactory epithelia of tiger salamanders selectively impairs detection of ketone-containing odorants. When a behavioral assay is used, decrements in responding to cyclopentanone or cyclohexanone are observed at the same time as responding to cyclopentanol, ethyl butyrate, or dimethyl disulfide is unaffected. Dose-response studies show an increase in duration (but not profundity) of selective hyposmia with increasing fixer concentration. On the other hand, the data show a much smaller increase in duration (and no increase in profundity) when the blocker concentration is increased. These results conform to expectations based on the expression for ϕ above. They are consistent with the supposition that olfactory ketone receptors with bound ligand behave as do rod cells in the retina in the dark: with a small molecule covalently attached by a Schiff base linkage and with continual secretion of neurotransmitter.

Covalent modification of proteins is a widely used tool for examining the action of enzymes.[2] Recently, this technique has been extended to the study of receptors in tissue samples. In vivo applications have been less widely probed, for most investigations have not required that the subject survive the chemical treatment. This paper describes the development of a two-step affinity labeling procedure suitable for treating olfactory epithelia of living animals. The two reagents used are a blocker, which binds reversibly to proteins, and a fixer, which converts the reversible complex to an irreversible adduct. Because the experimental subjects remain alive, their sense of smell can be assayed following treatment in order to assess whether the ability to detect specific classes of compounds has been impaired. This paper presents kinetic analyses for two-step labeling schemes, experimental tests using model proteins in solution, and results of application of a two-step labeling procedure to the noses of live tiger salamanders (*Ambystoma tigrinum*).

The perception of odors is an opportune field for chemical investigation.[3] There is no complete catalogue of olfactory sensations. Electrophysiological data (much of which has been recorded from salamanders)[4–6] do not reveal obvious patterns of coding nor is it known how many varieties of receptor sites exist. Snyder and co-workers have recently isolated an odorant-binding

(1) Portions of this work have been presented at the 14th Annual Meeting of the Society for Neuroscience, Anaheim, CA, Oct 1984, and at the 189th National Meeting of the American Chemical Society, Miami, FL, April 1985.

(2) (a) Fridovich, I.; Westheimer, F. H. *J. Am. Chem. Soc.* **1962,** *84,* 3208. (b) Grazi, E.; Rowley, P. T.; Cheng, T.; Tchola, O.; Horecker, B. L. *Biochem. Biophys. Res. Commun.* **1962,** *9,* 38–43. (c) Glazer, A. N.; DeLange, R. J.; Sigman, D. S. In "Laboratory Techniques in Biochemistry and Molecular Biology"; Work, T. S., Work, E., Eds.; Elsevier: New York, 1976; Vol. 4, pp 1–205. (d) Means, G. E. *Methods Enzymol.* **1977,** *47,* 469–478. (e) Plapp, B. V. *Methods Enzymol.* **1982,** *87,* 469–499.

(3) For a review of recent investigations, see: Cagan, R. H.; Kare, M. R. "Biochemistry of Taste and Olfaction"; Academic Press: New York, 1981.

(4) (a) Kauer, J. S. *J. Physiol. (London)* **1974,** *243,* 695–715. (b) Kauer, J. S.; Moulton, D. G. *J. Physiol. (London)* **1974,** *243,* 717–737. (c) Moulton, D. G. In "Odor Quality and Chemical Structure"; (Moskowitz, H. R.; Warren, C. B., Eds.) American Chemical Society: Washington, DC, 1981; ACS Symp. Ser. No. 148, pp 211–230.

(5) (a) Getchell, T. V. *Brain Res.* **1977,** *123,* 275–286. (b) Getchell, T. V.; Heck, G. L.; DeSimone, J. A.; Price, S. *Biophys. J.* **1980,** *29,* 397–405. (c) Masukawa, L. M.; Kauer, J. S.; Shepherd, G. M. *Neurosci. Lett.* **1983,** *36,* 59–64. (d) Trotier, D.; MacLeod, P. *Brain Res.* **1983,** *268,* 225–237.

(6) (a) Baylin, F. *J. Gen. Physiol.* **1979,** *74,* 17–36; (b) Baylin, F.; Moulton, D. G. *J. Gen. Physiol.* **1979,** *74,* 37–55.

[†] Monell Chemical Senses Center.
[‡] University of California.